

# Temperature–Time Texture Transition of $\text{Pb}(\text{Zr}_{1-x}\text{Ti}_x)\text{O}_3$ Thin Films: I, Role of Pb-rich Intermediate Phases

San-Yuan Chen\* and I-Wei Chen\*

Department of Materials Science and Engineering, University of Michigan, Ann Arbor, Michigan 48109-2136

Lead-rich intermediate phases, in particular  $\text{Pt}_{5-7}\text{Pb}$  and  $\text{PbO}$ , are found to form on Pt(111) atop Ti-buffered Si substrates prior to formation of  $\text{Pb}(\text{Zr}_{1-x}\text{Ti}_x)\text{O}_3$  (PZT) thin films.  $\text{Pt}_{5-7}\text{Pb}$  is a [111] textured transient intermetallic phase that nucleates PZT[111] texture.  $\text{PbO}$  is a [001] textured layer compound that nucleates PZT[100] texture. The formation conditions and lattice matching of these intermediate phases have been examined. The presence of other possible intermediate phases, such as pyrochlore and Zr and Ti-rich phases, has also been investigated but found unrelated to the texture selection of perovskite PZT.

## I. Introduction

THIN FILMS of  $\text{Pb}(\text{Zr}_{1-x}\text{Ti}_x)\text{O}_3$  (PZT) with preferred crystallographic orientations are currently being considered for applications in electro-optical devices, nonvolatile memory, and dynamic access memory.<sup>1,2</sup> Some recent studies have shown that different preferred orientations of Pb-based perovskite films can be obtained on a common substrate. For example, PZT films can be grown on Pt(111)/Ti/SiO<sub>2</sub>/Si<sup>3,4</sup> and sapphire.<sup>5</sup> Also  $\text{Pb}(\text{Mg}_{1/3}\text{Nb}_{2/3})\text{O}_3$  films with both [111] and [100] textures can be obtained from Pt(111)<sup>6</sup> substrate. The [111] and [100] textures emerge from these studies as the most preferred orientations. The development of [111] texture for perovskite on Pt(111) should come as no surprise. Perovskite has an  $\text{ABO}_3$  formula ( $A = \text{Pb}$  and  $B = \text{Zr/Ti}$  in PZT) in which  $\text{AO}_3$  forms a face-centered cubic sublattice. For PZT, the (111) planes of  $\text{AO}_3$  and Pt are reasonably well-matched, both having a hexagonal pattern with an interatomic spacing around 2.77 Å. The development of [100] texture, on the other hand, is less obvious. However, since the [100] texture can grow not only on Pt, but also on the other substrates such as sapphire ( $\text{Al}_2\text{O}_3$ )<sup>5,7</sup> and even fused silica, which is noncrystalline,<sup>8</sup> it might be regarded as one of the intrinsic habits of PZT growth. For a further understanding of these phenomena, the detailed mechanisms of texture selection and formation need to be identified. The present study describes a set of specially designed experiments that attempt to identify such mechanisms. In the companion paper,<sup>9</sup> we also identify, for metallorganic PZT solutions deposited on a Pt(111)/Ti/SiO<sub>2</sub>/Si substrate, the broad range of heat-treatment conditions that lead to the two textures. A temperature–time transformation texture (TTT) diagram is constructed to summarize such results,<sup>9</sup> and the shape of the transformation curves in the diagram suggests the operation of diffusion-controlled nucleation and growth reactions.

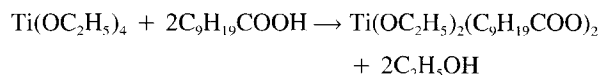
The texture selection and formation mechanisms are closely related to the composition and phase identity at the ceramic/

substrate interface. Since the organic solution undergoes complex decomposition and phase evolutions during pyrolysis and crystallization, it is necessary to definitively identify the critical step for interfacial phase formation that dictates the subsequent texture evolution. We recently reported an intermetallic Pt–Pb transient phase that forms epitaxially on the Pt(111) substrate.<sup>10</sup> Although this intermediate interfacial phase is only a transient phase, it leads to the selection of PZT [111] variant because of the good lattice matching between itself and the PZT variant. This finding has encouraged us to examine other possibilities of Pb-rich intermediate phases which may influence the selection and formation of PZT orientations. Simulation experiments which isolate the critical intermediate phases pertinent to subsequent texture evolution have been performed. The microstructural/kinetic model constructed from these experiments is applied in the companion paper to understand the various compositional and heat-treatment effects on texture development.

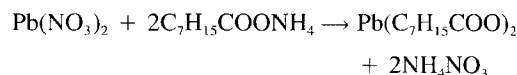
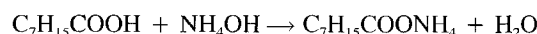
## II. Experimental Procedure

### (I) Preparation of Stock Solution

The precursor solutions used to prepare  $\text{Pb}(\text{Zr}_{0.52}\text{Ti}_{0.48})\text{O}_3$  were lead 2-ethylhexanoate ( $\text{Pb}(\text{C}_8\text{H}_{15}\text{O}_2)_2$ ), zirconium octoate ( $\text{Zr}(\text{C}_7\text{H}_{15}\text{COO})_4$ ) (commercial solution from Pfaltz & Bauer), and titanium-diethoxy-dineodecanoate ( $\text{Ti}(\text{OC}_2\text{H}_5)_2(\text{C}_9\text{H}_{19}\text{COO})_2$ ). Niobium triethoxy dineodecanoate ( $\text{Nb}(\text{OCH}_2\text{H}_5)_3(\text{C}_9\text{H}_{19}\text{COO})_2$ ) was also prepared. The general procedures used to fabricate titanium-diethoxy-dineodecanoate and lead 2-ethylhexanoate were described by Vest.<sup>11</sup> Titanium ethoxide liquid was first mixed with benzene, and then neodecanoate acid was added into the solution. The mixture solution was heated and refluxed for 5 h under nitrogen atmosphere to avoid the absorption of moisture from air. It was then subjected to distillation using a rotary vacuum. After that, xylene ( $\text{C}_8\text{H}_{10}$ ) was added to adjust the viscosity of the solution. The formula reaction is



The precursor to synthesize the niobium triethoxy dineodecanoate is niobium pentaethoxide, and the process is very similar to the one described above. For lead 2-ethylhexanoate, the 2-ethylhexanoic acid was first added to ammonium hydroxide to form an ammonium soap solution. Lead nitrate was dissolved in deionized water, then added dropwise into the ammonium soap to form a pale-yellow gummy substance. After that, xylene was added to dissolve the lead 2-ethylhexanoate. The formula reactions are



To determine the yield of these solutions, a known quantity of the solution calcined and the product oxide was weighed. The solutions were then mixed at various ratios to obtain preceramic PZT solutions of a given stoichiometry.

S.-I. Hirano—contributing editor

Manuscript No. 193950. Received December 21, 1993; approved May 27, 1994. Supported by the U.S. Department of Energy (BES) under Grant No. DE-FG02-87ER45302.

\*Member, American Ceramic Society.

## (2) Preparation of Thin Films

Thin films were fabricated on silicon wafers and Pt(111)/Ti/SiO<sub>2</sub>/Si substrates by spin coating. The viscosity of the solution was around 4.5 cps, and a single coating was used. After deposition, samples were placed into a preheated tube furnace, held at 300° to 700°C for various times, and rapidly withdrawn afterwards. Typically, after full pyrolysis, a crack-free film ranging from 0.1 to 0.3- $\mu$ m thickness was obtained. To evaluate the effect of oxidation conditions, both air and a gas mixture (2% O<sub>2</sub> and 98% Ar) were used in the above procedure. Typically, the PZT films produced were of the composition Pb(Zr<sub>0.52</sub>Ti<sub>0.48</sub>)O<sub>3</sub>. In addition, we evaluated the effect of a thin pure oxide (PbO, TiO<sub>2</sub>, and ZrO<sub>2</sub>) buffer coating (0.05  $\mu$ m) between PZT and Pt. A single thick PbO layer and a single Pb<sub>2</sub>Nb<sub>2</sub>O<sub>7</sub> pyrochlore layer were also separately studied.

## (3) Characterization

The phase and orientation of the films were determined by standard  $\theta$ - $2\theta$  and asymmetric  $\theta_0$ - $2\theta$  X-ray diffraction (XRD) methods. In the latter method,  $\theta_0$  was set at 5° and  $2\theta$  was scanned to reveal reflections from crystallographic planes not parallel to the substrate surface. Both the microstructure and the thickness of the films were examined using scanning electron microscopy (SEM). Differential thermal analysis (DTA) and thermogravimetry (TG) were performed to provide supplementary information of phase evolution.

## III. Results and Discussion

### (1) Pb-Pt Intermetallic and PZT [111] Orientation

An epitaxial Pt<sub>5.7</sub>Pb phase was identified in our previous work for PZT films heated over a wide temperature range but for a very short time (e.g., 600°C for 2.5 min).<sup>10</sup> This intermetallic phase was found to precede the formation of perovskite [111] texture. To isolate the source of this intermediate phase, we coated lead 2-ethylhexanoate solution to a Pt(111)/Ti/SiO<sub>2</sub>/Si substrate and followed its pyrolysis using XRD. As shown in Fig. 1, PbO (both tetragonal and orthorhombic structures) and Pt<sub>5.7</sub>Pb (fcc structure) reflections are identified in the XRD patterns after 2 min at 550°C in O<sub>2</sub>-Ar atmosphere. The above XRD pattern was obtained using the  $\theta$ - $2\theta$  method in which the highly [111] textured Pt<sub>5.7</sub>Pb phase produced only one reflection at 38.5° ( $d = 2.34$  Å). This corresponds to the (111) diffraction plane of an fcc cell of a lattice parameter  $a_0 = 4.05$  Å. Using the asymmetric diffraction method, we also obtained other allowable reflections for an fcc lattice with the above lattice parameter.<sup>10</sup>

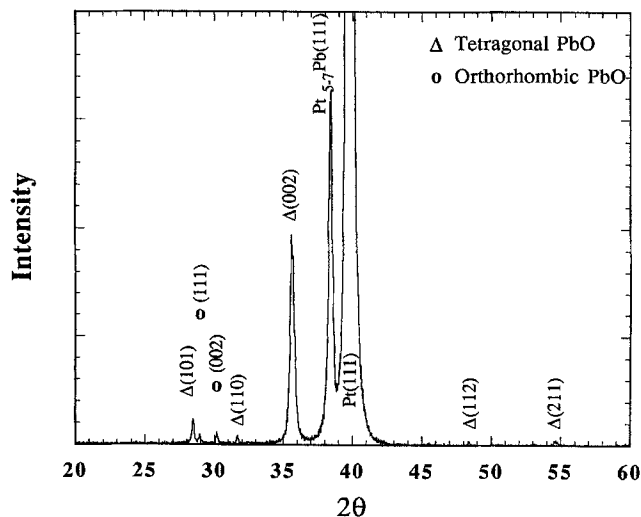


Fig. 1. XRD pattern of PbO film on Pt(111)/Ti/SiO<sub>2</sub>/Si substrate (heated at 550°C for 2 min in 2% O<sub>2</sub>-Ar).

The behavior diagram of Pt<sub>5.7</sub>Pb phase formation is constructed in Fig. 2 for two atmospheres, air and 2% O<sub>2</sub>-Ar. As is evident in Fig. 2, the formation regime of Pt<sub>5.7</sub>Pb is narrower in air than in 2% O<sub>2</sub>-Ar. This is because both lead 2-ethylhexanoate and Pt<sub>5.7</sub>Pb are easier to oxidize in air. Indeed, the Pt<sub>5.7</sub>Pb phase is only a transient phase, stable for a short period of time.<sup>9</sup> It forms by reducing Pb<sup>2+</sup> to Pb, which can be effected at a relatively high P<sub>O<sub>2</sub></sub>, around 10<sup>-5</sup> atm, between 400° and 700°C. (This estimate is based on an Ellingham diagram.<sup>12</sup>) This modestly reducing atmosphere can be attained because of the depletion of oxygen within the ceramic film during the initial stages of pyrolysis, when oxygen intake from the atmosphere has not yet reached very far beneath the film outer surface. Since the condition is most reducing at the buried ceramics/Pt interface, the Pt<sub>5.7</sub>Pb intermetallic forms there first. Over time, oxygen intake from the atmosphere reoxidizes Pb back to Pb<sup>2+</sup>, and the intermetallic phase disappears.

We also investigated single coatings of titanium-diethoxydineodecanoate and zirconia octoate on the substrate and followed their pyrolysis. Under the same set of conditions as described above, no intermediate compounds other than the expected TiO<sub>2</sub> (amorphous or both rutile and anatase) and ZrO<sub>2</sub> (amorphous or tetragonal) phases were found. This can be understood from the same thermodynamic consideration above, because both Ti and Zr are much more difficult to reduce. The partial pressure of O<sub>2</sub> required for Ti<sup>4+</sup> → Ti is 10<sup>-13</sup> atm and for Zr<sup>4+</sup> → Zr even lower.<sup>12</sup> (Thermodynamic data for this reaction are not available.) These extreme reducing conditions are not likely to be attained during pyrolysis in air or in a slightly reducing atmosphere.

The Pt-Pb epitaxial layer was also found in the early stage pyrolysis of PZT films. Its importance to the PZT texture is illustrated in Fig. 3 for a PZT coating, which clearly shows that the PZT[111] orientation follows that of Pt<sub>5.7</sub>Pb[111]. From the relative peak positions, it is also evident that a good matching of  $d$ -spacing is obtained between Pt ( $a_0 = 3.922$  Å), Pt<sub>5.7</sub>Pb ( $a_0 = 4.050$  Å) and PZT ( $a_0 = 4.077$  Å). Since all three compounds are fcc or fcc-like, we can expect good matching on their (111) planes. For further comparison, the behavior diagram of Pt<sub>5.7</sub>Pb formation in air for the PZT film reported in Ref. 7 is replotted in Fig. 4. The close resemblance of Figs. 2 and 4 leaves no doubt that the phase in question is Pb-rich. The PZT[111] texture is thus controlled by the formation of the Pt<sub>5.7</sub>Pb intermetallic.

### (2) PbO/Pyrochlore and PZT(100) Orientation

The formation of a tetragonal PbO compound occurs above 300°C. This is verified by coating lead 2-ethylhexanoate onto a Pt(111)/Ti/SiO<sub>2</sub>/Si substrate, followed by pyrolysis and XRD. A series of diffraction patterns at increasing temperatures is

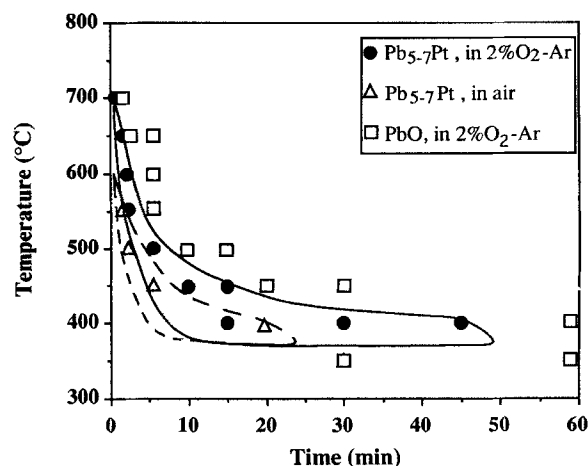


Fig. 2. TTT diagram for Pt<sub>5.7</sub>Pb phase formation on Pt(111)/Ti/SiO<sub>2</sub>/Si substrate. Solid curve for 2% O<sub>2</sub>-Ar and broken curve for air.

shown in Fig. 5. At higher temperatures, the dominant phase is the orthorhombic type. At even higher temperatures, PbO reacts with the substrate and the (PbO)<sub>o</sub> reflections disappear. It is also found that for both (PbO)<sub>o</sub> and (PbO)<sub>t</sub>, the [001] texture is favored. The behavior diagram of these phase evolutions is shown in Fig. 6.

The presence of a PbO layer on the Pt(111)/Ti/SiO<sub>2</sub>/Si substrate has a definitive effect on the texture of the PZT overlayer. To demonstrate this effect, we prepared samples with a thin (0.05 μm) coating of lead 2-ethylhexanoate, then pyrolyzed them at 400°C for 1 h to obtain PbO, then recoated them with the metallorganic solution corresponding to PZT stoichiometry, and finally pyrolyzed them again using two heating schedules. For comparison, samples without the first PbO layer were also prepared and heat treated using the same schedules. The first schedule used was 400°C for 0.5 h, then 650°C for 0.5 h. As shown in Fig. 7(a), this produces a strong PZT[100] texture with and without the PbO buffer. The second heating schedule used was annealing at 650°C for 0.5 h without intermediate pyrolysis at the lower temperature. From past experience, this heat treatment consistently favors a strong PZT[111] texture. Indeed, in the PZT film without the PbO buffer, this produces a strong PZT[111] texture, as shown in Fig. 7(b). With the PbO buffer, however, the PZT(111) peak is much weaker, and a strong PZT[100] texture is obtained instead. Thus the PbO buffer favors PZT[100] texture and suppresses PZT[111] texture.

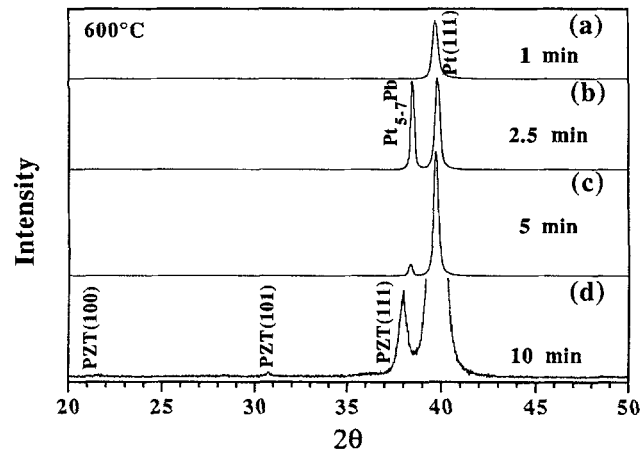


Fig. 3. XRD pattern of PZT film heated at 600°C for different times.

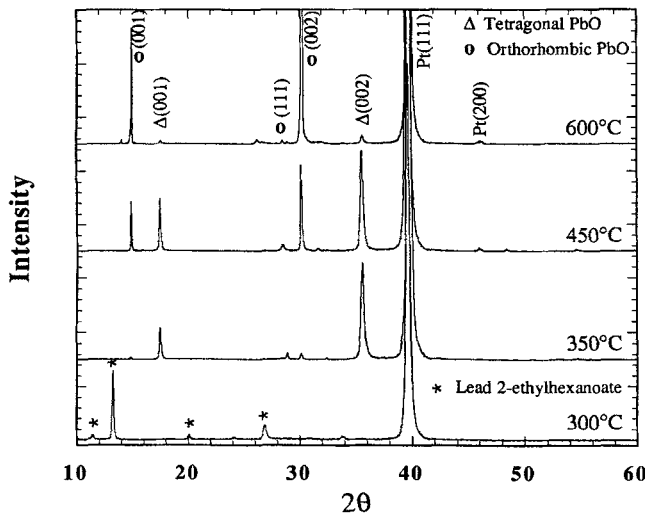


Fig. 5. XRD patterns of PbO films held at different temperatures for 1 h.

Evidence for PbO formation in pyrolyzing the metallorganic solution of the PZT stoichiometry was found using DTA. As shown in Fig. 8, solvent and organic evaporation/decomposition is largely complete at around 350°C. Toward the end of this process, a small but sharp endothermic peak at 325°C can be identified. Powders heated to just above this temperature showed (PbO)<sub>o</sub> reflections in XRD and no other crystalline phase reflections. In fact, the formation of PbO was actually followed by another organic decomposition peak at 350°C, then pyrochlore formation over a broad temperature range at around 430°C, before the final appearance of a perovskite phase above 500°C. In thin films, these reaction temperatures are believed to be somewhat different but should follow the same sequence.

Broad pyrochlore reflections were readily identified on the films with the PZT composition pyrolyzed above 400°C for sufficient time (5 min to 2 h). Unlike PbO, pyrochlore reflections were not sharp enough to allow texture identification. The broadening in this case is usually attributed to the small crystallite sizes and the broad compositional range over which pyrochlore is expected to form. Pyrochlore crystallites cannot be coarsened enough before their disappearance because of the formation of PZT in this system. Hence, it is difficult to ascertain their effect on PZT texture. However, we also prepared a specimen with a solution corresponding to Pb<sub>2</sub>Nb<sub>2</sub>O<sub>7</sub> stoichiometry. Since Pb<sub>2</sub>Nb<sub>2</sub>O<sub>7</sub> is also a pyrochlore of the same cubic structure as Pb<sub>2</sub>Ti<sub>2</sub>O<sub>6</sub> that presumably exists in PLT/PZT system (*a* = 10.40 Å for Pb<sub>2</sub>Ti<sub>2</sub>O<sub>6</sub> and 10.508 Å for Pb<sub>2</sub>Nb<sub>2</sub>O<sub>7</sub>),<sup>13</sup> it

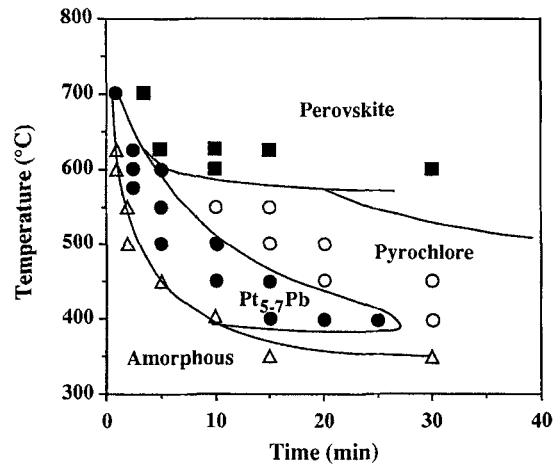


Fig. 4. TTT diagram for crystallization of PZT films on Pt(111)/Ti/SiO<sub>2</sub>/Si substrate.

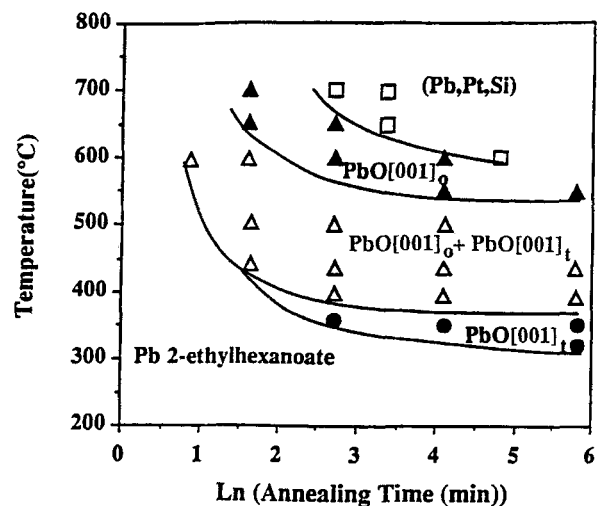


Fig. 6. TTT diagram for PbO phase formation.

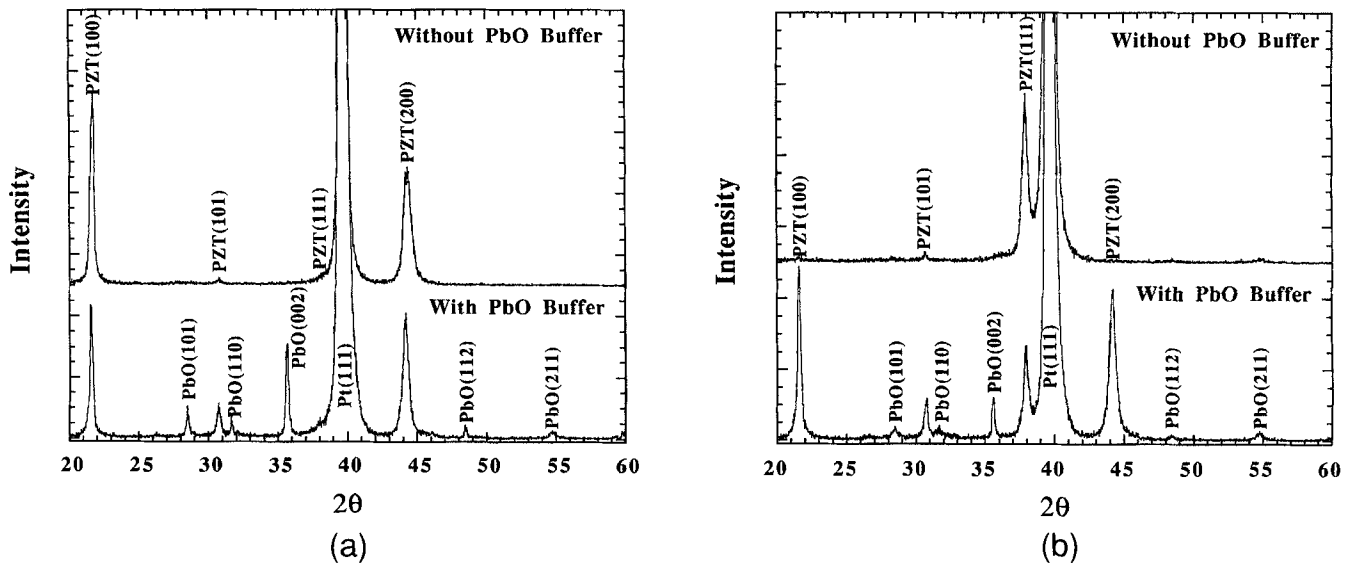


Fig. 7. Effect of PbO buffer layer on texture formation of PZT films (a) pyrolyzed at 400°C and then fast annealed at 650°C, and (b) fast heated directly to 650°C.

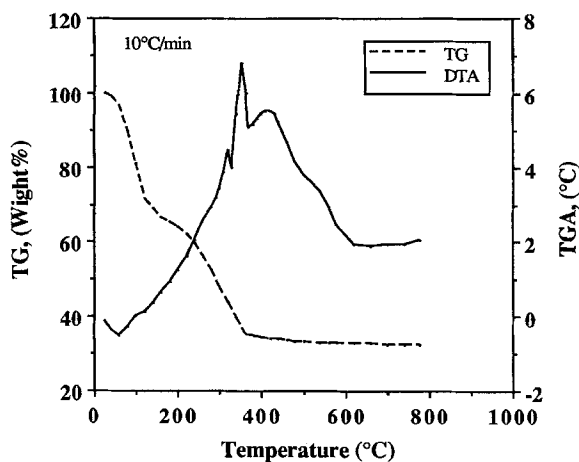


Fig. 8. DTA and TGA curves of PZT precursor solution. Heating rate = 10°C/min.

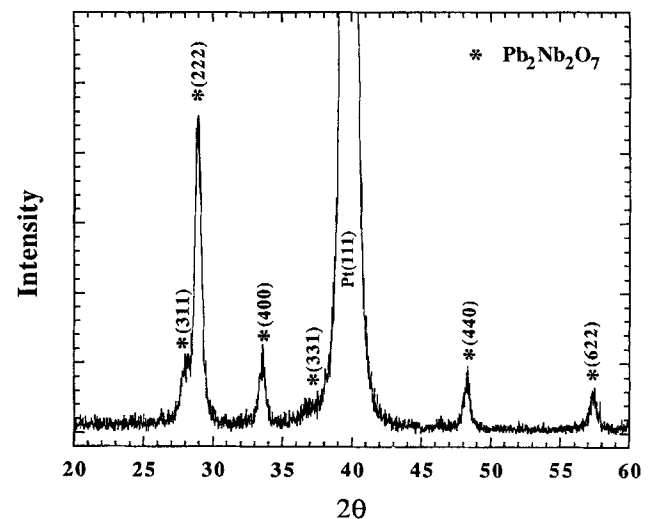


Fig. 9. XRD pattern of  $\text{Pb}_2\text{Nb}_2\text{O}_7$  on Pt(111)/Ti/SiO<sub>2</sub>/Si substrate.

can be used to simulate the  $\text{Pb}_2\text{Ti}_2\text{O}_6$  texture. Figure 9 shows the XRD pattern of a  $\text{Pb}_2\text{Nb}_2\text{O}_7$  film heated to 750°C. The pattern matches well with that of  $\text{Pb}_2\text{Ti}_2\text{O}_6$ <sup>14</sup> and is nearly indistinguishable from that of powder diffraction patterns of the same composition, indicating the lack of texture. Assuming the same for  $\text{Pb}_2\text{Ti}_2\text{O}_6$ , we suggest that the PZT[100] texture is related to PbO and not inherited from pyrochlore, even though the latter always precedes PZT[100] formation.

### (3) Model for Texture Formation

Based on the above observations, we now propose a model that rationalizes the formation of intermediate phases and final textures. First, the PZT[111] texture forms on the Pt<sub>5-7</sub>Pb buffer layer. This intermetallic phase is epitaxial with Pt(111) substrate and has good lattice matching with PZT(111), as shown in Fig. 10(a). The formation condition requires either firing in a reducing atmosphere or rapid heating to high temperatures. Otherwise, oxidation of the intermetallic film takes place before the perovskite PZT has time to grow onto the buffer layer. Second, the PZT[100] texture forms on the PbO buffer layer. The PbO(001) plane matches reasonably well with that of PZT(100) ( $a_0 = 3.9723$  Å for O-sublattice in PbO versus  $a_0 = 4.05$  Å for O or cation sublattices in PZT), as shown in Fig. 10(b). The origin of PbO[001] texture is attributed to the layerlike structure of this compound which contains Pb with lone-pair electrons.

(Note the large off-plane  $c$ -spacing (5.019 Å) because of Pb.) The formation condition is not stringent, and PbO tends to be the first phase formed on the substrate at lower temperature, leading to subsequent PZT[100] selection. Third, pyrochlore forms at a lower temperature than perovskite but does not have a special texture and probably does not originate from the substrate interface. It has a lattice structure which does not provide any special plane for good matching with PZT(100). It is also rather ionic in nature and has little tendency to grow in a layer-like pattern. Therefore, it has no influence on the selection of PZT texture and will decompose at higher temperature to reform perovskite PZT.

Additional microstructural observations are noted below. Typically, the formation of PZT[111] on Pt<sub>5-7</sub>Pb can occur easily, and the microstructure of the PZT[111] film obtained is rather uniform with good transparency. The PbO coverage on the Pt-Si substrate, however, is not very uniform. The PZT[100] crystal habit is probably heterogeneously nucleated onto PbO(001) at many sites, and these nuclei spread out radially into the matrix, which is already partially decomposed into pyrochlore, until impingement. The microstructure of the PZT[100] film obtained thus contains more grain boundaries and porosity. Lastly, we found that, after long annealing, other

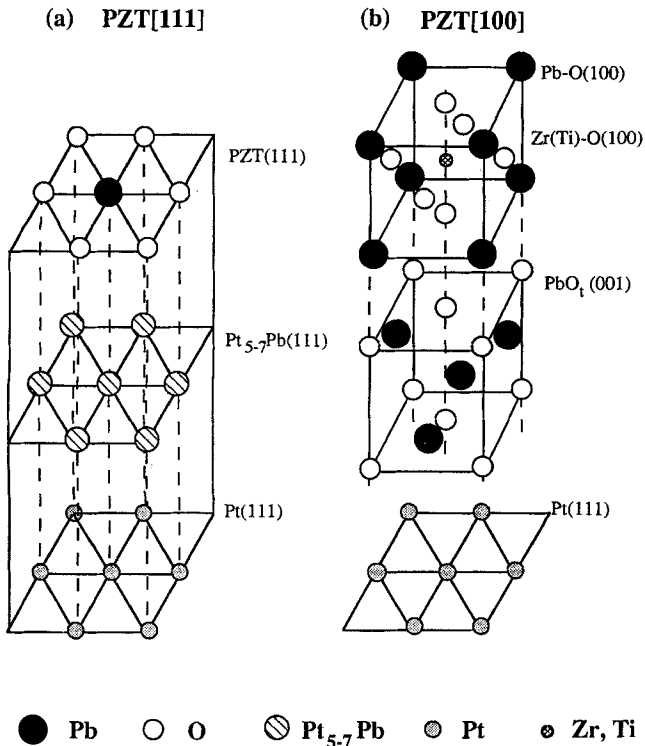


Fig. 10. Schematic structure of PZT films and substrate for (a) [111] and (b) [100] texture.

PbO orientations began to form, especially if PbO evaporated. Thus, PbO[001] texture is not stable against prolonged heat treatments. These microstructural features are discussed in the companion paper.<sup>9</sup>

#### IV. Conclusions

(1) An intermetallic phase of good lattice matching with Pt(111) precedes the formation of PZT(111). This intermetallic phase is definitely Pb-rich and not related to Ti or Zr. XRD

identifies it as Pt<sub>5.7</sub>Pb. This phase is transient and forms under reducing atmosphere.

(2) PbO is a layer compound that forms readily on a Pt/Si substrate that has a [001] texture at lower temperatures. It provides a good lattice-matching substrate for forming PZT(100). The PbO[001] texture is unstable after prolonged annealing.

(3) Pyrochlore rich in Pb and Ti is not textured and does not provide lattice-matching planes for nucleating either [100] or [111] perovskite textures.

#### References

- <sup>1</sup>S. L. Swartz, "Topics in Electronic Ceramics," *IEEE Trans. Electr. Insul.*, **25** [5] 935-87 (1990).
- <sup>2</sup>L. H. Parker and A. F. Tasch, "Ferroelectric Materials for 64 Mb and 256 Mb Drams," *IEEE Circuits Devices Mag.*, **6** [1] 17-26 (1990).
- <sup>3</sup>T. Tani, Z. Xu, and D. A. Payne, "Preferred Orientations for Sol-Gel Derived PLZT Thin Layers," *Mater. Res. Soc. Symp. Proc.*, **310**, 269-74 (1993).
- <sup>4</sup>M. Klee, R. Eusemann, R. Waser, and W. Brand, "Processing and Electrical Properties of Pb(Zr<sub>x</sub>Ti<sub>1-x</sub>)O<sub>3</sub> ( $x = 0.2-0.75$ ) Films: Comparison of Metallo-Organic Decomposition and Sol-Gel Processes," *J. Appl. Phys.*, **72** [4] 1566-76 (1992).
- <sup>5</sup>D. Xiao, J. Zhu, J. Zhu, Z. Xiao, Z. Qian, and H. Zhang, "The Orientation of (Pb,La)TiO<sub>3</sub> Thin Films Grown on Different Substrates by Multi-Ion-Beam Reactive Co-sputtering Technique," *Ferroelectrics*, **141**, 327-33 (1993).
- <sup>6</sup>K. Okuwada, M. Imai, and K. Kakuno, "Preparation of Pb(Mg<sub>1/3</sub>Nb<sub>2/3</sub>)O<sub>3</sub> Thin Film by Sol-Gel Method," *Jpn. J. Appl. Phys.*, **29**, L1271-73 (1989).
- <sup>7</sup>J. Xu and R. W. Vest, "Preparation and Properties on PLZT Films from Metallo-Organic Precursors," *Ferroelectrics*, **93**, 21-29 (1989).
- <sup>8</sup>A. Y. Wu, D. M. Hwang, and L. M. Wang, "Highly Oriented (Pb,La)-(Zr,Ti)O<sub>3</sub> Thin Films on Amorphous Substrates," pp. 301-304 in *Proceedings of the 8th IEEE International Symposium on Applications of Ferroelectrics* (Greenville, SC), Edited by M. Liu, A. Safari, A. Kingon, and G. Haertling. IEEE, New York, 1992.
- <sup>9</sup>S. Y. Chen and I-W. Chen, "Temperature-Time-Texture Transition of Pb(Zr,Ti)O<sub>3</sub> Thin Films: II. Heat Treatment and Compositional Effects," *J. Am. Ceram. Soc.*, **77** [9] 2337-44 (1994).
- <sup>10</sup>S. Y. Chen and I-W. Chen, "Phase Transformations of Orientation Pb(Zr<sub>1-x</sub>Ti<sub>x</sub>)O<sub>3</sub> Thin Films from Metallo-Organic Precursors," *Ferroelectrics*, **152** [124] 25-30 (1994).
- <sup>11</sup>R. W. Vest, "Electronic Films from Metallo-Organic Precursors," pp. 303-41 in *Ceramic Films and Coating*, Edited by J. B. Wachtman and R. A. Haber. Noyes Publications, Park Ridge, NJ, 1993.
- <sup>12</sup>L. S. Darken and R. W. Gurry, *Physical Chemistry of Metals*, p. 349. McGraw-Hill, New York, 1953.
- <sup>13</sup>Y. Shimizu, K. R. Udayakumar, and L. E. Cross, "Preparation and Electrical Properties of Lanthanum-Doped Lead Titanate Thin Films by Sol-Gel Processing," *J. Am. Ceram. Soc.*, **74** [12] 3023-27 (1991).
- <sup>14</sup>F. Martin, "A Metastable Cubic Form of Lead Titania Nucleated Glass Ceramics," *Phys. Chem. Glasses*, **6** [4] 143-46 (1965). □